

## **On the dominance of pre-existing swells over wind seas along the west coast of India**

V.M. Aboobacker\*<sup>1</sup>, R. Rashmi<sup>1</sup>, P. Vethamony<sup>1</sup>, H.B. Menon<sup>2</sup>

<sup>1</sup>National Institute of Oceanography (CSIR), Dona Paula, Goa - 403004, India

<sup>2</sup>Department of Marine Science, Goa University, Taleigao Plateau, Goa – 403206, India

\* Corresponding author: V.M. Aboobacker, email: [vmabacker@gmail.com](mailto:vmabacker@gmail.com)

### **Abstract**

Wave data collected off Goa along the west coast of India during February 1996 – May 1997 has been subject to spectral analysis, and swell and wind sea parameters have been estimated by separation frequency method. Dominance of swells and wind seas on monthly and seasonal basis has been estimated, and the analysis shows that swells dominate Goa coastal region not only during southwest monsoon (93%), but also during the post-monsoon (67%) season. Wind seas are dominant during the pre-monsoon season (51%). The mean wave periods ( $T_m$ ) during southwest monsoon are generally above 5 s, whereas  $T_m$  is below 5 s during other seasons. Co-existence of multiple peaks (from NW and NE) was observed in the locally generated part of the wave spectrum, especially during the post-monsoon season. NCEP reanalysis winds have been used to analyze active fetch available in the Indian Ocean, from where the predominant swells propagate to the west coast of India. A numerical model was set up to simulate waves in the Indian Ocean using flexible mesh bathymetry. The correlation coefficients between measured and modelled significant wave heights and mean wave periods are 0.96 and 0.85, respectively. Numerical simulations reproduced the swell characteristics in the Indian Ocean, and from the model results potential swell generation areas are identified. The characteristics of swells associated with tropical storms that prevailing off Goa during 1996 have also been analysed.

## 1. Introduction

Swells in the Indian Ocean vary in response to the prevailing wind systems according to the seasons: pre-monsoon (February – May), southwest (SW) monsoon (June – September) and post-monsoon (October - January). The sea state along the coastal regions of India is significantly modified by these swells (Kumar et al., 2009). Identification of potential swell generation areas during various seasons is important to understand the effect of swells along the Indian coast where they superimpose with coastal wind seas and create complex sea states. Along the west coast of India swells are predominant during SW monsoon (Kumar et al., 2000). However, during the pre-monsoon season, wind seas play a major role in controlling the wave characteristics (Rao and Baba, 1996). Sea-breeze is very active during pre-monsoon season (Aparna et al., 2005), and it has an impact on the diurnal cycle of sea state along the west coast of India (Neetu et al., 2006). Co-existence of locally generated wind seas and pre-existing swells results in a diurnal pattern of wave parameters during the pre-monsoon season (Vethamony et al., 2009). This can significantly affect the design of offshore structures, ship passages, small boat operations in the harbor entrance and sea-keeping safety (Earle, 1984). Shamal swells are generated in the northwestern Arabian Sea due to strong NW winds (called shamal winds) during winter shamal events which occur during post-monsoon and early pre-monsoon seasons (Aboobacker et al., 2011). They propagate in the Arabian Sea with mean wave period ranges between 6 and 8 s, affecting the west coast of India significantly.

The spectra along the Indian coast are generally multi-peaked (e.g., Harish and Baba, 1986; Rao and Baba, 1996; Kumar et al., 2003) and occurrences of double-peaked spectra are more frequent during low sea states (Sanil Kumar et al., 2004). Spectra during extreme events are single-peaked (Kumar et al., 2004; Aboobacker et al., 2009). This occurs when spectral peak period ( $T_p$ ) for fully developed sea equals peak wave period ( $T_p$ ) (Torsethaugen and Haver, 2004). Wind sea dominance occurs when  $T_p < T_{pf}$ , where the spectral peak is in the high frequency region, and swell dominance occurs when  $T_p > T_{pf}$ , where the spectral peak is in the low-frequency region.

Identification and separation of wind sea and swell energies from the measured spectra allow us to have a more realistic description of the sea state (Wang and Hwang, 2001). Kumar et al. (2000) used the cut off frequency (determined based on spectral density curve, mean direction and beam width) method to estimate wind sea and swell parameters and studied wind sea and swell characteristics during the southwest monsoon season along the west coast of India. Wang and Hwang (2001) used a separation frequency,  $f_s$  based on wave steepness to distinguish between wind seas and swells. Wave

components with frequencies greater than  $f_s$  are generated by local winds and those with frequencies lesser than  $f_s$  are from distant swells. Portilla et al (2009) used the partitioning scheme to separate wind sea and swell from the wave energy spectra; they found that the method of Wang and Hwang (2001) tends to overestimate swells, especially during wind sea dominated conditions. Gilhousen and Hervey (2001) calculated separation frequency by assuming that wind seas are steeper than swells and that maximum steepness occurs in the wave spectrum near the peak of wind sea energy. This method improved the swell estimates significantly, and subsequently, this method has been implemented by the National Data Buoy Centre (NDBC), NOAA, USA. Violante-Carvalho et al. (2004) calculated sea-swell parameters from measured spectral data and studied wind sea and swell characteristics at Campos Basin in the South Atlantic.

The present study aims at: (i) understanding monthly and seasonal scenarios of wind sea and swell characteristics and dominance of wind sea and swell along the west coast of India, and (ii) reproducing the swell in the Indian Ocean during various seasons and extreme weather events using numerical simulations and identifying potential swell areas which affect the west coast of India. For this purpose, wave data obtained from field measurements, and numerical results were analysed.

## **2. Area of study**

Goa is situated on the west coast of India with a shoreline orientation of approximately  $15^\circ$  to the north and facing the Arabian Sea (Fig. 1). Wave measurement location is at 23m water depth and approximately 11 km away from the coast. The climate along the west coast of India varies according to the seasons. Wave pattern is characterized by the influence of wind systems associated with seasons: pre-monsoon, SW monsoon and post-monsoon. Wave heights are generally very high during the southwest monsoon season and low during pre-monsoon and post-monsoon seasons. The frequency of extreme events is less in the Arabian Sea compared to those in the Bay of Bengal. Whenever such events occur in the Arabian Sea, especially during southwest monsoon and post monsoon (also called NE monsoon) seasons, significant wave heights reach upto 6 m and the impact of these events was significant along the nearshore regions.

## **3. Data and methods**

The wave energy spectra and wave parameters obtained at 23m water depth off Goa ( $15^\circ 27.9'$  N and  $73^\circ 41'$  E) during February 1996 to May 1997 have been analyzed to study primarily the wind sea - swell characteristics along the west coast of India. Wave measurements were carried out for 20

minutes duration at 3 hour interval using a Datawell Directional Wave Rider Buoy (Datawell, 2006). The frequency range of the measured wave spectra is 0.025 - 0.58 Hz. The frequency associated with peak energy in the spectrum indicates the dominant wave system over the region at that time.

The wind sea and swell parameters have been separated using the methodology given by Gilhousen and Hervey (2001), which is based on wave steepness algorithm. The wave steepness parameter,  $\zeta$ , at all frequencies  $f$ , can be written as,

$$\zeta(f) = \frac{2\pi H_s(f)}{g T_m(f)} \dots \dots \dots (1)$$

where,  $H_s$  (significant wave height) and  $T_m$  (mean wave period) are functions of a given frequency  $f$ . When wave spectrum components are expressed in terms of moments of the distribution, the overall  $\zeta(f)$  calculated above for a given frequency  $f_i$  can be rewritten as,

$$\zeta(f_i) = \frac{8\pi \int_{f_i}^{f_u} f^2 E(f) df}{g \sqrt{\int_{f_i}^{f_u} E(f) df}} \dots \dots \dots (2)$$

where,  $E(f)$  is the wave variance spectrum,  $f_u$  (=0.58 Hz) and  $f_i$  (= 0.03, 0.04,....0.58 Hz) are the upper and lower frequency limits of the considered part of the spectrum, and  $g$  is acceleration due to gravity. Using Eqn.(2),  $\zeta(f)$  has been calculated for all frequencies from the measured data ( $f_u$  is fixed for all calculations and  $f_i$  varies in such a way that  $f_i = f_1, f_2, \dots, f_u$ ). The frequency  $f_x$  (peak frequency), corresponding to the maximum steepness parameter  $\zeta(f)$ , has been used to calculate the separation frequency  $f_s$ , as follows:

$$f_s = C f_x \dots \dots \dots (3)$$

where  $C = 0.75$  is an empirically determined constant (Gilhousen and Hervey, 2001).

The methodology proposed by Wang and Hwang (2001) has been applied to study the sensitivity of the results obtained from the separation frequency method of Gilhousen and Hervey (2001). Fig. 2 shows the comparison of separation frequencies obtained from both the methods, and the match is very good.

The wave parameters such as significant wave height ( $H_s$ ), mean wave period ( $T_m$ ) and mean wave direction ( $\theta$ ) have been calculated for the wind sea and swell after dividing the spectra into wind sea and swell parts. In case multiple peaks are present within the separated wind sea and swell spectra, they are treated as single wind sea or swell system.  $H_s$  and  $T_m$  are calculated using equation (4) as given below:

$$H_s = 4\sqrt{m_0(f)}, \quad T_m = \sqrt{\frac{m_0(f)}{m_2(f)}} \dots \dots \dots (4)$$

Where,  $m_0$  and  $m_2$  are the zeroth and second moment of the wave variance spectrum, respectively,

$$m_n = \int_{f_l}^{f_u} f^n E(f) df \dots \dots \dots (5)$$

$f_l$  and  $f_u$  are the lower and upper frequencies for wind sea and swell spectra, respectively. Significant wave heights of wind sea, swell and total sea are related by:

$$H_s = \sqrt{H_{s\text{swell}}^2 + H_{s\text{sea}}^2} \dots \dots \dots (6) \text{ (WMO, 1998)}$$

NCEP reanalysis winds available for 2.5° x 2.5° grids at 6-hour interval (Kalney et al., 1996) have been analyzed to study the wind pattern of the Arabian Sea. Wind vectors at locations closer to Goa have been extracted during February 1996 to May 1997 and correlated with wind sea heights. NCEP winds and JTWC (Joint Typhoon Warning Center) storm tracks were analyzed to study the associated wind sea and swell characteristics..

Model domain (Indian Ocean) covers the region bounded by 65°S to 30°N (latitude) and 20° to 125°E (longitude), and simulations have been carried out using MIKE 21 SW, a spectral wave model developed by DHI Water & Environment, Denmark (DHI, 2009). Several studies have been carried out along the Indian coast using this model (e.g., Vethamony et al., 2006; Kurian et al., 2009; Aboobacker et al., 2009). Growth, decay and transformation of wind seas and swells are taken care of in the model. The discretization of the governing equation in geographical and spectral space is performed by the cell-centered finite volume method. The time integration is performed using a fractional step approach, wherein a multi-sequence explicit method is applied for the propagation of wave action. An unstructured triangulated mesh is generated with varying size of the triangles: 1.5° (south Indian Ocean), 0.75° (northern Indian Ocean) and 0.25° (coastal region). ETOPO5 bathymetry data obtained from NGDC (National Geophysical Data Center, Colorado, USA) is applied to deep water regions and the data modified by Sindhu et al. (2007) to shallow water regions, and these are interpolated to each element in the unstructured mesh. Fig. 3 shows the model domain, flexible mesh and bathymetry. NCEP wind vectors (U and V components) have been applied as input parameter to the wave model. These winds were previously used to simulate waves in the Indian Ocean and to study wave characteristics at select locations along the Indian coast (Vethamony et al., 2009; Aboobacker et al., 2009). The modelled wave parameters ( $H_s$ ,  $T_m$  and  $\theta$ ) were stored for every 3-hour interval and the model results have been validated with the measurements.

## **4. Results and discussion**

The analysis shows that wave energy spectra, in general, consist of two/multiple energy peaks - one in the low frequency region (associated with swell) and the other(s) in the high frequency region (associated with locally generated seas) indicating the presence of two or more distinct wave systems prevailing in the region. The frequency range of primary and secondary peaks in the spectra varies according to the dominance of different wave systems. During extreme events, the spectra were mostly single-peaked.

### **4.1. Seasonal characteristics of wind seas and swells**

We present the seasonal scenarios of the nearshore wave characteristics, in addition to the observations made by Kumar and Anand (2004). The time series of  $H_s$ ,  $T_m$  and  $\theta$  of the total sea, swell and wind sea during the period from Feb 1996 to May 1997 are shown in Fig. 4. The maximum observed  $H_s$  is 5.85 m and the corresponding  $T_m$  is 9.1 s. The corresponding figures for swell and wind sea are 5.53 m / 2.3 m and 11.3 s / 4.8 s, respectively. The waves are predominantly

from SW, WSW and NW directions; swells from SW (27%), NW (23%) and WSW (20%) constitute 70% of the total swells, and wind seas from NW (41%), W (20%) and WNW (16%) constitute 77% of the total wind seas. The mean wave periods during southwest monsoon were generally above 5 s, whereas it is below 5 s during pre-monsoon and post-monsoon seasons (Fig. 4).

Waves during the SW monsoon season primarily follow the swell pattern, and energy associated with the swells is much higher than that of wind seas (Fig. 4). The swell heights are relatively higher than the wind sea heights during the post-monsoon season, while the opposite is true during the pre-monsoon season. The swell heights during pre-monsoon and post-monsoon seasons are nearly the same, except during storm events (October). The relatively higher wind sea heights during the pre-monsoon season are due to sea breeze activity. In the diurnal cycle the wind seas are dominant only during the active sea breeze period (Vethamony et al., 2011). As sea breeze weakens, the sea conditions decay progressively and revert back to the swell conditions.

Monthly variations in  $H_s$  and  $T_m$  of swell and wind sea are presented in Table 1. Maximum wind sea and swell  $H_s$  were observed during June and July. The swell  $H_s$  was very low ( $< 1.0$  m) during November, December, February and April, whereas wind sea  $H_s$  was low ( $< 1.0$  m) during November and December. The Maximum swell mean period ( $= 13.8$  s) was observed during December, whereas the maximum wind sea mean period ( $= 6.2$  s) was observed during September. The corresponding minimum values were observed (swell, 5.1 s) during February and (wind sea, 2.0 s) during December and January.

Fig. 5 shows the monthly mean and standard deviation of wind sea and swell parameters. Monthly mean swell heights were below 0.5 m from November to February, between 0.5 and 0.7 m during March to May, between 0.9 and 1.0 m during September and October and upto 2.5 m during June - August. Monthly mean wind sea heights were below 0.4 m during November and December, between 0.4 and 0.7 m during January - May and September - October and between 0.9 and 1.1 m during June - August. Though it is the post-monsoon season, the average swell heights during October were higher due to two unusual tropical storms/depressions that affected the region. Otherwise, mean swell heights during post-monsoon season are relatively lower compared to pre-monsoon season (Fig. 5). Monthly mean swell periods were between 7.0 and 8.0 s during September - March and May, and between 8.0 and 10.0 s during June - August and April. Monthly mean wind

sea periods were below 3.5 s during October - May and between 3.5 to 4.0 s during June - September.

Fig. 6 shows a typical one-dimensional (1D) wave energy spectrum with mean wave direction for each frequency and wind rose off Goa during pre-monsoon, SW monsoon and post-monsoon seasons. The predominant winds are: from NW, NNW and N during pre-monsoon season, from WSW, W and WNW during SW monsoon season (swells are mainly from W/WSW) and from NNW and E during post-monsoon season. However, the predominant wind seas are from SW/WSW during SW monsoon season and from NW (this is attributed to the local sea breeze, which is nearly absent in the coarse resolution of NCEP winds) during pre- and post-monsoon seasons. At several occasions, the high energy peak from the NW (generated locally at a nearby area of the measurement location due to NW winds) is accompanied with low energy peak from NE (generated within the region due to the NE winds, as visible in the NCEP winds) in the wind sea spectrum, especially during NE monsoon (Fig. 6c). Although not frequent, similar multiple peaks were found during the post-monsoon season. In general, the wave energy spectra measured off Goa during fair weather season (pre-monsoon and post-monsoon) are composed of swell from a predominant direction and locally generated seas from one or more directions. Identification and separation of multi-directional peaks in the wind sea part of the spectrum demands an advanced algorithm that separates each peak with respect to its direction. The presently available separation/partitioning algorithms (Gilhousen and Hervey, 2001; Wang and Hwang, 2001; Portilla et al., 2009; etc.) divide the wave energy spectrum into two parts (swell and wind sea). However, the secondary peaks within the divided spectrum (swell or wind sea part) are usually merged, irrespective of the direction of each peak. Under changing winds (both magnitude and direction) wave systems overlap in the frequency direction domain, which are difficult to identify by automated procedures (Portilla et al, 2009).

Separation of multi-directional peaks in the wind sea spectrum would help in understanding the characteristics of the light wind seas present in the spectrum. In the present study, the low wind seas observed are mainly from NE due to the NE monsoon winds prevailing over the region. However, light winds are produced in the atmospheric marine boundary layer due to an upward momentum transfer from long period swells (Hogstrom et al., 2009; Semedo et al., 2009; Smedman et al., 2009) which in turn generate light wind seas in the direction of the swells. The present data shows the presence of such light wind seas (from SW/SSW) at several occasions. In fact, a detailed analysis on the above aspect is in progress.



## 4.2. Dominance of wind sea and swell

Monthly dominance of swell and wind sea is presented in Table 2. Swells are predominant (above 50 % in heights) during March to December, and wind seas are predominant during January and February. Even though swells are predominant during March to May, November and December, the role of wind seas is significant (the percentage dominance of wind seas is above 30 % during the above months), since the co-existence of wind seas and swells result in complex sea states at nearshore areas. Maximum swell dominance (100 %) is observed during June to July, and maximum wind sea dominance (63 %) is observed during February. Annually, 70% of the waves are dominated by swells. Swells are predominant during SW monsoon and post-monsoon seasons (93 % and 67 %, respectively), whereas, wind seas are predominant during pre-monsoon season (51 %). Even though wind seas contributed sufficiently to the resultant wave, swell contribution exceeds that of seas due to the arrival of SW monsoon swells during SW monsoon season. The swell contribution is higher than that of wind sea during post-monsoon season, and hence the waves follow nearly the same pattern of swells.

Fig. 7a shows the locations of NCEP winds extracted in the Arabian Sea and Fig. 7b shows wind speed and direction off Goa (at W1) during February 1996 – May 1997. The selected locations are at 72.5° E, 15° N (W1); 65° E, 12.5° N (W2) and 55° E and 5° N (W3). The NCEP winds at W1 during February 1996 – May 1997 have been used to analyse the correlation with wave parameters. At W1, wind direction varies according to the seasons - between west-southwest (WSW) and north (N) during pre-monsoon, between northwest (NW) and east (E) during post-monsoon and between SW and NW during southwest monsoon. When multi-directional peaks (from NW and NE) were present in the wind sea spectrum, during which as mentioned above the NCEP shows only the presence of NE winds, the wind sea direction gives poor match with wind direction. These winds (NE) could affect the propagation of swells towards the southwestern Arabian Sea.

The complicated structure of the local wind sea or waves generated in close by areas is evident in the relatively large scatter around the best-fit line between NCEP wind speed and wind sea  $H_s$  (Fig. 8a). The correlation coefficient between wind speed and wind sea  $H_s$  is 0.72. This indicates that major part of the local wind contribution to the wind sea generation off the Goa coast has been captured in the NCEP winds, even though sea breeze (from NW) were absent during the post-monsoon season (Fig. 8b). There exist two distinct wind directions: (i) between SW and N and (ii) between N and E. Wind seas are primarily between SW and N. Though there exist winds between N and E, wind seas

from these directions are not visible due to the co-existence of multi-directional sea peaks associated to waves generated either locally or in nearby areas, as the energy from NW were predominant. Also, there is not sufficient fetch at the wave measurement location (close to the coast) for the winds between N and SSE to generate wind seas from these directions, as the winds are blowing from the land (shoreline orientation is approximately  $15^\circ$  to the north). Detailed investigation on the contribution of local winds to the generation of wind seas in the coastal regions demands the use of fine resolution (both temporal and spatial) wind fields, which were not available during the measurement period.

The offshore extension of the local winds controls the wind sea generation mechanism along the west coast of India. The winds during pre-monsoon season are dominated by sea breeze and their maximum seaward extension is 180 km off Goa (Aparna et al., 2005). Neetu et al., (2006) observed that sea breeze generated wind seas have considerable amount of energy in the wave spectra. Similar conditions prevail off the coast of Sydney, Australia, where the sea breeze produces 1 – 1.5 m high waves with periods ranging between 6 and 9 s (Masselink and Pattiaratchi, 1998). Recent studies on the wave characteristics off Goa coast during pre-monsoon season reveal systematic variations in significant wave heights and mean wave periods primarily due to superimposition of wind seas generated by sea breeze and pre-existing swells (Vethamony et al., 2011). The present study supports their findings extending the measurements to other seasons (the data during pre-monsoon 1996 and pre-monsoon 1997 clearly shows similar variations).

### **4.3. Model validation**

Simulated wave parameters are validated using measurements done during the period Feb 1996 – May 1997. Fig. 9 shows the comparison between measured and modelled wave parameters ( $H_s$  and  $T_m$ )s. Given the coarse input winds, poorly related to the local winds, we consider the fit between the measured and modelled wave (resultant) parameters as sufficiently satisfactory, particularly in the low value range. Table 3 provides correlation coefficient, bias, r.m.s. error and scatter index estimated between measured and modelled  $H_s$  and  $T_m$ . The correlation coefficient between measured and modelled  $H_s$  is 0.96 and between measured and modelled  $T_m$  is 0.85. Modelled significant wave height is slightly under-estimated with a bias of 0.06 m. The r.m.s. errors for  $H_s$  and  $T_m$  are 0.25 m and 0.8 s, respectively, and the scatter indices are 0.25 and 0.17, respectively.

Swell  $H_s$  is well predicted in the model domain, even though  $T_m$  gives poor correlation. The correlation coefficient between the measured and modelled swell  $H_s$  and  $T_m$  are 0.93 and 0.45, respectively. Even though the correlation coefficient for swell  $T_m$  is low, the bias between the measurements and modelling are negligible (bias = -0.2 s). The wind seas are not well predicted (correlation coefficient for  $H_s$  is 0.64 and for  $T_m$  is 0.28) in the coastal region off Goa. This limitation is due to coarse resolution of NCEP winds, wherein local wind effects near the coast are not well represented.

#### **4.4. Potential swell generation regions**

##### **4.4.1. Wave observations**

In order to identify potential generation areas of the swells reaching the Goa coast, wind patterns at 3 cells, namely, W1, W2 and W3 (Fig. 7a) have been analysed. During SW monsoon season, wind direction at W3 is predominantly between SW and WSW, at W2, between SW and W with dominating WSW direction and at W1, between SW and NW with dominating W direction. However, the swells off Goa are predominantly between WSW and W with dominating WSW direction during June – Sept. This indicates that the potential swell generation area during SW monsoon season is between W3 and W2, probably around 60° E and 10° N.

During the pre-monsoon season, winds at W3 are predominantly between NNE and E in February – April and between SW and WNW in May; at W2, between N and NE in February – March and between W and NE in April – May, and at W1, between W and N with dominant NW direction. However, two distinct swells (SW/SSW and NW) were present during the pre-monsoon season. The mean periods associated with SW/SSW swells are predominantly 8 to 11 s, whereas, those associated with NW swells are 6 to 8 s. Swells generated by the winds from N, NE and E do not concern the west coast of India. Since SW/SSW winds are not prevalent in the north Indian Ocean (as observed at W1, W2 and W3) during pre-monsoon season, it is possible that they are generated in the south Indian Ocean. The analysis of wind pattern over the south Indian Ocean indicates that these swells are generated at the mid-latitudes, probably around 40° S, where strong SW/SSW winds are always present. NW winds are stronger in the northwestern Arabian Sea during winter shamal events. Shamal swells propagate to the Goa coast with a deep water group velocity of approximately 9 m/s (Aboobacker et al., 2011).

During the post-monsoon season, winds at W3 and W2 are predominantly between N and E, and at W1 between NW and E. Similar to the observations during pre-monsoon season, there are two distinct swells: SW/SSW and NW swells (shamal swells). The mean periods associated with SW swells are 8 to 12 s, whereas those associated with NW swells are 6 to 8 s. The long-period SW/SSW swells are generated in the south Indian Ocean, whereas NW swells are generated in the northwestern Arabian Sea.

#### **4.4.2. Numerical model results**

Numerical simulations indicate that the predominant swells off the west coast of India are from SW/SSW and NW directions during pre-monsoon and post-monsoon seasons and from SW and WSW directions during SW monsoon season. Fig. 10 shows the typical swell patterns in the Indian Ocean during pre-monsoon and post-monsoon seasons. NW swells are stronger during the post-monsoon season as compared to those during the pre-monsoon season. The swell heights are below 2.0 m along the west coast of India during the above seasons. It has been found that the SW/SSW swells are generated in an area covered by 40° E to 70° E and 30° S to 50° S and propagate towards the west coast of India as long-period swells during pre-monsoon and post-monsoon seasons. During the SW monsoon season, the swell height reaches upto 4.0 m along the west coast of India. The simulations indicate that the predominant swells during SW monsoon season are generated in an area covered by 52.5° E to 62.5° E and 5° N to 15° N.

From Fig. 9, it is evident that modelled wave parameters follow reasonably well the measurements. Certainly enough to use the model data to derive an indication of the wave height distribution along the west coast of India. Hence, modelled wave parameters at various locations (Fig. 1) have been extracted and analysed for their distributions. Fig. 11 shows the modelled significant wave heights at 25m depth off Kochi, Mangalore, Goa, Ratnagiri and Mumbai during pre-monsoon, SW monsoon and post-monsoon seasons. It has been found that the significant wave height follows nearly the same pattern at all locations though there are time lags due to different arrival times of the swells. This gives an indication that swell dominates during SW monsoon and post-monsoon seasons, and wind sea dominates during pre-monsoon season all along the west coast of India and their distribution (% of swell and wind sea) is relatively the same at all locations as observed in the Goa region.

#### 4.5. Wave characteristics during tropical storms

Joint Typhoon Warning Center (JTWC) reported two extreme events (15 -25 June 1996 and 14 October – 2 November 1996) in the Arabian Sea in 1996. These are subtropical storms of Category 1 with maximum wind speed of 34 m/s. The first storm developed at an offshore location of Goa; it moved towards north, and changed its direction towards west, and finally hit the Gujarat coast after 3 days. The maximum intensity of the storm was on 19 June 1996, and weakened while travelling towards the subcontinent. The second storm developed in the Bay of Bengal, moved across the subcontinent towards west and crossed the region between Goa and Mangalore. The maximum speed was observed off Ratnagiri (approx. 200 km north of Goa) on 23 October 1996.

Gridded NCEP winds show that wind speeds in the Arabian Sea are of the order of 20 – 34 m/s during the tropical storms (i) 15 -25 June 1996 and (ii) 14 October – 2 November 1996). During evolution of the storms, a gradual increase in wave height is observed along with an increase in wave period (Fig. 4). Following the peak intensity of the event, maximum  $H_s$  of 5.85 m and 3.32 m and maximum  $T_m$  of 9.1 s and 6.8 s were observed for the storms (i) and (ii), respectively. The swell  $H_s$  are nearly the same as that of total sea and the waves follow the pattern of swells. The correlation coefficient between swell  $H_s$  and resultant  $H_s$  is 0.99, whereas, correlation coefficient between wind sea and resultant swell  $H_s$  during both the storm events is 0.87. Since storm-1 is associated with SW monsoon, the propagation direction of the waves remained the same (SW). Prior to storm-2, the predominant wave direction was W. However, on the evolution of the storm, the wave direction had changed to SSW, and further to SW, following a sudden shift in the cyclone track.

Measured and modelled significant wave heights show very good match during the tropical storm events. For storm-1, the correlation coefficients between measurements and modelling for total  $H_s$ , swell  $H_s$ , and wind sea  $H_s$  are 0.93, 0.79 and 0.74, respectively, whereas they are 0.80, 0.74 and 0.7, respectively for storm-2. The swells of storm-1 resemble the same pattern (in terms of propagation direction) of the SW monsoon swells, and they are in different directions (mainly SSW and SW directions) for storm-2. Off Goa, the significant swell heights are above 6.5 m (Fig. 12) and the mean swell periods are of the order of 11 -13 s for storm-1. The resultant wave reaches maximum  $H_s$  of 7.9 m at an offshore location off Ratnagiri during storm-1 and 3.6 m off Mumbai during storm-2.

## **5. Conclusions**

The wind seas and swells off Goa have been separated from the measured wave spectra using the separation frequency method and monthly and seasonal characteristics have been discussed. The waves off Goa primarily follow the swell pattern during most part of the year. The dominance of swells during southwest monsoon, post-monsoon and pre-monsoon seasons are 93%, 67% and 49%, respectively. Wind sea energy dominates over swell energy during pre-monsoon season. Even though wind seas contributed significantly to the resultant wave, swell contribution exceeded that of wind sea due to the arrival of SW swells during SW monsoon season. Wind sea contribution is relatively low during post-monsoon season, and hence distant swells (SW/SSW direction) dominate along the west coast of India. Multi-directional peaks (from NW and NE) in the wind sea part of the spectrum were present during pre-monsoon and post-monsoon seasons. Analysis of waves during tropical storms reveals that waves off Goa coast are primarily dominated by SW swells.

Numerical simulations reproduced the swell characteristics off the west coast of India. Predominant swells are from SW direction during SW monsoon season and from SW/SSW and NW directions during both pre-monsoon and post-monsoon seasons. The potential swell generation areas are identified as follows: (i) area covered by  $52.5^{\circ}$  E to  $62.5^{\circ}$  E and  $5^{\circ}$  S to  $15^{\circ}$  S for SW swells during SW monsoon season and (ii) area covered by  $40^{\circ}$  E to  $70^{\circ}$  E and  $30^{\circ}$  S to  $50^{\circ}$  S for SW/SSW swells during pre-monsoon and post-monsoon seasons. Though waves during SW monsoon season have very high impact on the west coast of India, the wind seas super-imposed on pre-existing swells do cause geomorphological changes during non-monsoon months.

## **Acknowledgements**

We thank Dr S.R. Shetye, Director, National Institute of Oceanography (NIO), Goa for providing necessary facilities and constant encouragement. We acknowledge all the project participants, especially Mr. K. Ashok Kumar, Mr. P. Pednekar and Mr. Manohar Mochemadkar for their help during wave data collection. This study is carried out as a part of partial fulfillment of Ph.D. work of the first author. The NIO contribution number is xxxx.

## References

- Aboobacker, V.M., Vethamony, P., Rashmi, R., 2011. "Shamal" swells in the Arabian Sea and their influence along the west coast of India. *Geophys. Res. Lett.* 38, L03608, doi:10.1029/2010GL045736.
- Aboobacker, V.M., Vethamony, P., Sudheesh, K., Rupali, S.P., 2009. Spectral characteristics of the nearshore waves off Paradip, India during monsoon and extreme events. *Natural Hazards* 49, 311–323.
- Aparna, M., Shetye, S.R., Shankar, D., Shenoi, S.S.C., Mehra, P., Desai, R.G.P., 2005. Estimating the seaward extent of sea breeze from QuikSCAT scatterometry. *Geophys. Res. Lett.* 32, L13601, doi:10.1029/2005GL023107.
- Datawell BV, 2006. Datawell wave rider reference manual. Datawell BV, Zumerlustraart 4, 2012 LM Haarlem, The Netherlands.
- DHI, 2009. MIKE 21 SW, User Manual. DHI Water & Environment, Denmark.
- Earle, M.D., 1984. Development of Algorithms for separation of sea and swell. National Data Buoy Centre Tech. Rep. MEC-87-1, 53 pp.
- Gilhousen, D.B., Hervey, R., 2001. Improved Estimates of Swell from Moored Buoys. Proceedings of the Fourth International symposium WAVES 2001, ASCE: Alexandria, VA. 387-393.
- Harish, C.M., Baba, M., 1986. On spectral and statistical characteristics of shallow water waves. *Ocean Eng.* 13(3), 239–248.
- Hogstrom, U., Smedman, A., Sahlee, E., Drennan, W.M., Kahma, K.K., Pettersson, H., Zhang, F., 2009. The atmospheric boundary layer during swell: a field study and interpretations of the turbulent kinetic energy budget for high wave ages. *Journal of the Atmospheric Sciences* 66, 2764-2779.
- Kumar, R., Bhowmick, S.A., Ray, S., Bhatt, V., Surendran, S., Basu, S., Sarkar, A., Agarwal, V.K., 2009. Improvement in predictability of waves over the Indian Ocean. *Natural Hazards* 49, 275-291.
- Kumar, V.S., Ashok Kumar, K., Anand, N.M., 2000. Characteristics of waves off Goa, west coast of India. *Journal of Coastal Research* 16(3), 782-789.
- Kumar, V. S., Anand, N.M., Kumar, K.A., Mandal, S., 2003. Multi peakedness and groupiness of shallow water waves along Indian coast. *Journal of Coastal Research* 19, 1052-1065.
- Kumar, V.S., Anand, N.M., 2004. Variation in wave direction estimated using first and second order Fourier coefficients. *Ocean Engineering* 31, 2105-2119.
- Kumar, V.S., Ashok Kumar, K., Raju, N.S.N., 2004. Wave characteristics off Visakhapatnam coast during a cyclone. *Current Science* 86, 1524–1529.
- Kurian, N.P., Rajith, K., Shahul Hameed, T.S., Sheela Nair, L., Ramana Murthy, M.V., Arjun, S., Shamji. V.R., 2009. Wind waves and sediment transport regime off the south-central Kerala coast, India. *Natural Hazards* 49, 325-345.

- Masselink, G., Charithra, B.P., 1998. The effect of sea breeze on beach morphology, surf zone hydrodynamics and sediment resuspension. *Marine Geology* 146, 115-135.
- Neetu, S., Shetye, S.R., Chandramohan, P., 2006. Impact of sea-breeze on wind-seas off Goa, west coast of India. *Journal of Earth System Science* 115(2), 229-234.
- Portilla, J., Ocampo-Torres, F.J., Monbaliu, J., 2009. Spectral partitioning and identification of wind sea and swell. *Journal of Atmospheric and Oceanic Technology* 26, 107-122.
- Rao C.V.K.P., Baba, M., 1996. Observed wave characteristics during growth and decay: a case study. *Cont. Shelf Research* 16(12), 1509–1520.
- Semedo, A., Saetra, O., Rutgersson, A., Kahma, K.K., Pettersson, H., 2009. Wave-induced wind in the marine boundary layer. *Journal of the Atmospheric Sciences* 66, 2256-2271.
- Sindhu, B., Suresh, I., Unnikrishnan, A.S., Bhatkar, N.V., Neetu, S., Michael, G.S., 2007. Improved bathymetric data sets for the shallow water regions in the Indian Ocean. *Journal of Earth System Science* 116(3), 261-274.
- Smedman, A., Hogstrom, U., Sahlee, E., Drennan, W.M., Kahma, K.K., Pettersson, H., Zhang, F., 2009. Observational study of marine atmospheric boundary layer characteristics during swell. *Journal of the Atmospheric Sciences* 66, 2747-2763.
- Torsethaugen, K., Haver, S., 2004. Simplified double peak spectral model for ocean waves. *Proceedings of ISOPE conference* 3, 76–84.
- Vethamony P., Aboobacker, V.M., Sudheesh, K., Babu, M.T., Ashok Kumar, K., 2009. Demarcation of inland vessels' limit off Mormugao Port region, India: a pilot study for the safety for inland vessels using wave modelling. *Natural Hazards* 49, 411–420.
- Vethamony P., Sastry, J.S., 1986. On the characteristics of multi-peaked spectra of ocean surface waves. *J Inst Eng India* 66, 129–132.
- Vethamony, P., Sudheesh, K., Rupali, S.P., Babu, M.T., Jayakumar, S., Saran, A.K., Basu, S.K., Raj Kumar, Abhijit Sarkar, 2006. Wave modelling for the north Indian Ocean using MSMR analysed winds. *International Journal of Remote Sensing* 27(18), 3767-3780.
- Vethamony, P., Aboobacker, V.M., Menon, H.B., Ashok Kumar, K., Cavaleri, L., 2011. Superimposition of wind seas on pre-existing swells off Goa coast. *Journal of Marine Systems* 87(1), 47-54.
- Violante-Carvalho, N., Ocampo-Torres, F.J., Robison, I.S., 2004. Buoy observations of the influence of swell on wind waves in the open ocean. *Applied Ocean Research* 26, 49-60.
- Wang, D.W. and P.A. Hwang (2001): An operational method for separating wind sea and swell from ocean wave spectra. *Journal of Atmospheric and Oceanic Technology* 18, 2052-2062.
- WMO (1998): Guide to wave analysis and forecasting. World Meteorological Organisation, WMO-No. 702, 159 pp.



## Table captions

Table 1 Monthly variations (minimum and maximum) of  $H_s$  and  $T_m$  for the **swell and wind sea**.

Table 2 Monthly percentage dominance of swell and wind sea.

Table 3 Correlation coefficient, bias, r.m.s. error and scatter index estimated between measured and modelled  $H_s$  and  $T_m$ .

## Figure captions

Fig. 1. Study area and measurement location

Fig. 2. Comparison of separation frequencies obtained from ‘Gilhousen and Harvey’ and ‘Wang and Hwang’ methodologies: (a) SW monsoon, (b) post-monsoon and (c) pre-monsoon.

Fig. 3. Model domain, bathymetry and unstructured mesh used for wave simulations.

Fig. 4. Distribution of (a) significant wave height, (b) mean wave period and (c) mean wave direction for the total sea, swell and wind sea during the period from February 1996 to May 1997.

Fig. 5. Monthly mean and standard deviation of swell and wind sea parameters: (a) significant wave height and (b) mean wave period.

Fig. 6. Typical 1D wave energy spectra with mean direction for each frequency and wind rose during (a) pre-monsoon, (b) SW monsoon and (c) post-monsoon seasons.

Fig. 7. (a) Locations of NCEP wind extracted and (b) wind speed and direction at W1 (off Goa) during Feb 1996 to May 1997.

Fig. 8. Scatter diagrams (a) wind speed vs. wind sea  $H_s$  and (b) wind direction vs. wind sea direction.

Fig. 9. (a) Comparison between measured and modelled  $H_s$ , (b) comparison between measured and modelled  $T_m$ , (c) scatter between measured and modelled  $H_s$  and (d) scatter between measured and modelled  $T_m$ .

Fig. 10. Typical swell patterns in the Indian Ocean during (a) pre-monsoon season (12 April 1997) and (b) post-monsoon season (10 December 1996).

Fig. 11. Significant wave heights off Kochi, Mangalore, Goa, Ratnagiri and Mumbai during (a) pre-monsoon, (b) SW monsoon and (c) post-monsoon seasons.

Fig. 12. Wave height distribution during tropical storm in the Arabian Sea.

## Tables

Table 1 Monthly variations (minimum and maximum) of  $H_s$  and  $T_m$  for the swell and wind sea.

Parameters	Significant wave height (m)		Mean wave period (s)	
	Swell	Sea	Swell	Sea
January	0.16 - 1.10	0.13 - 1.56	5.3 - 11.3	2.0 - 4.9
February	0.16 - 0.94	0.16 - 1.27	5.1 - 11.9	2.1 - 4.9
March	0.20 - 1.50	0.19 - 1.50	5.6 - 12.7	2.1 - 5.1
April	0.13 - 0.97	0.10 - 1.27	5.7 - 12.3	2.1 - 4.9
May	0.28 - 1.13	0.20 - 1.10	6.0 - 12.7	2.1 - 5.1
June	0.75 - 5.53	0.31 - 2.30	7.3 - 11.3	2.5 - 5.6
July	1.04 - 3.87	0.44 - 1.81	7.5 - 11.3	2.9 - 5.4
August	0.53 - 2.18	0.37 - 1.74	6.7 - 11.0	2.6 - 6.1
September	0.18 - 1.77	0.28 - 1.28	6.3 - 12.2	2.3 - 6.2
October	0.33 - 3.22	0.15 - 1.50	5.8 - 11.5	2.2 - 6.1
November	0.21 - 0.87	0.11 - 0.88	5.5 - 13.0	2.1 - 5.0
December	0.16 - 0.76	0.11 - 0.80	5.4 - 13.8	2.0 - 5.7

Table 2 Monthly percentage dominance of swell and wind sea.

Month	Swell (%)	Wind sea (%)
January	48.5	51.5
February	36.8	63.2
March	55.7	44.3
April	50.5	49.5
May	52.9	47.1
June	99.6	0.4
July	100.0	0.0
August	87.0	13.0
September	85.7	14.3
October	87.9	12.1
November	60.0	40.0
December	69.6	30.4

Table 3 Correlation coefficient, bias, r.m.s. error and scatter index estimated between measured and modelled  $H_s$  and  $T_m$ .

Parameters	Resultant		Swell		Wind sea	
	$H_s$	$T_m$	$H_s$	$T_m$	$H_s$	$T_m$
Correlation coefficient	0.96	0.83	0.93	0.45	0.64	0.28
Bias (m)	0.06	0.1	-0.07	-0.2	0.31	0.3
r.m.s. error (m)	0.29	0.8	0.36	2.5	0.46	1.6
Scatter Index	0.25	0.17	0.39	0.32	0.7	0.49

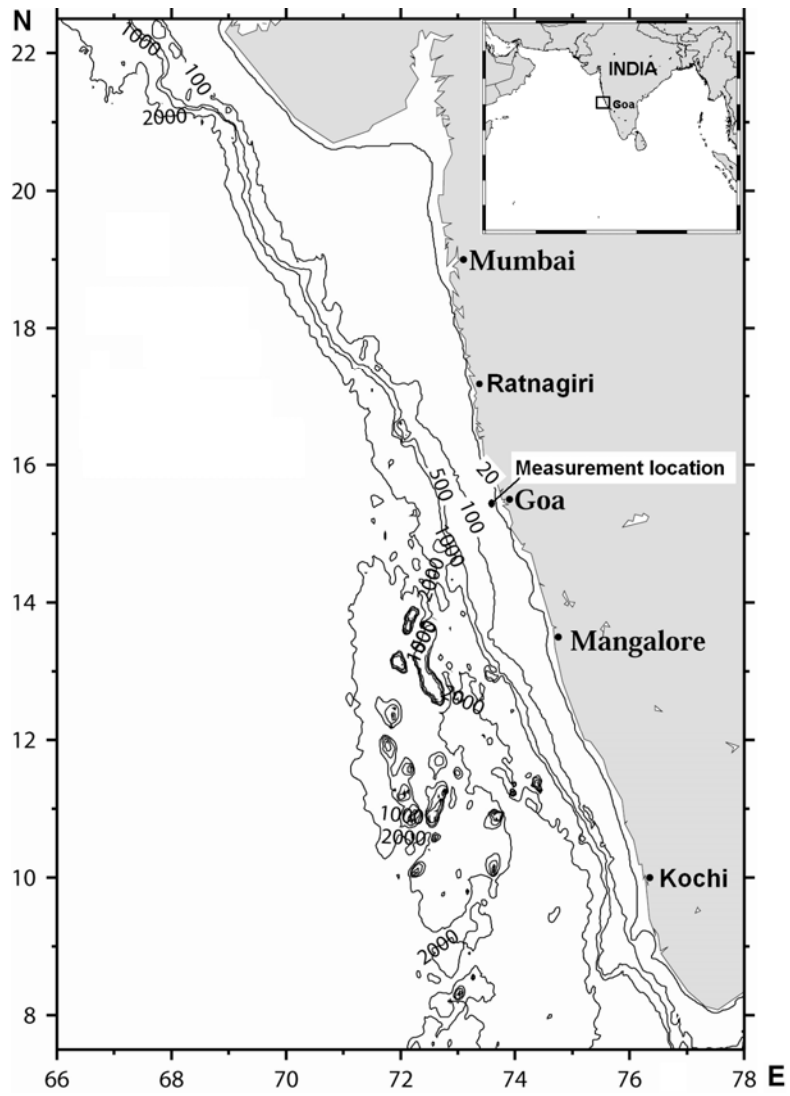


Figure 1

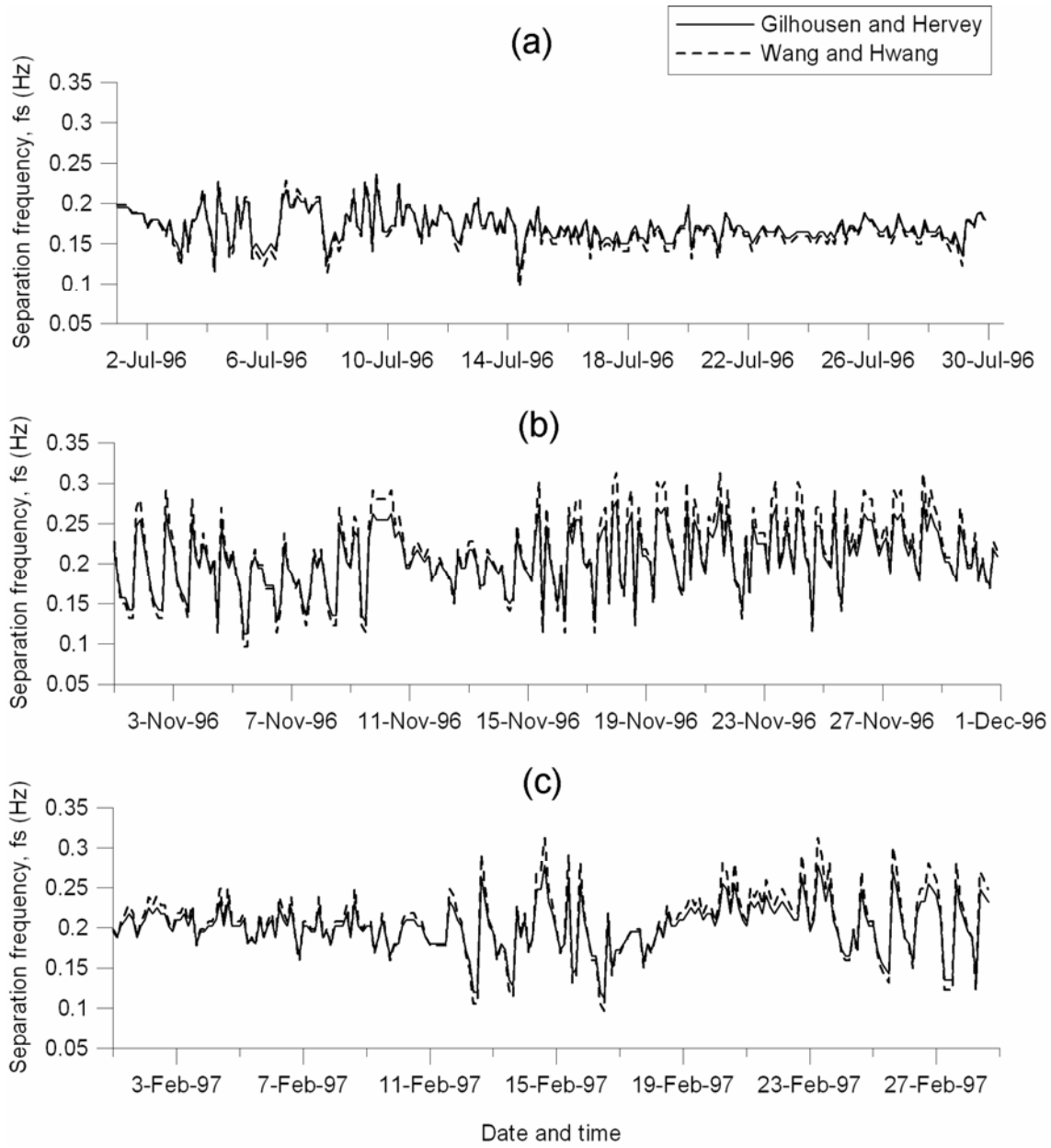


Figure 2

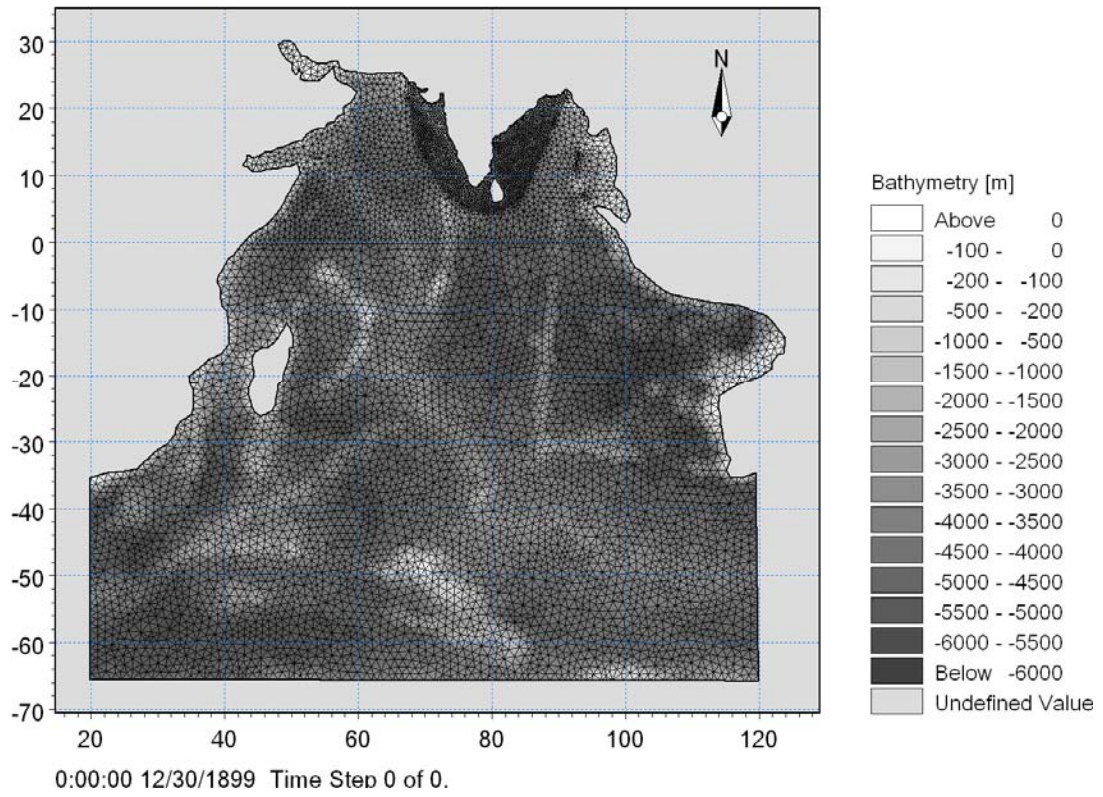


Figure 3



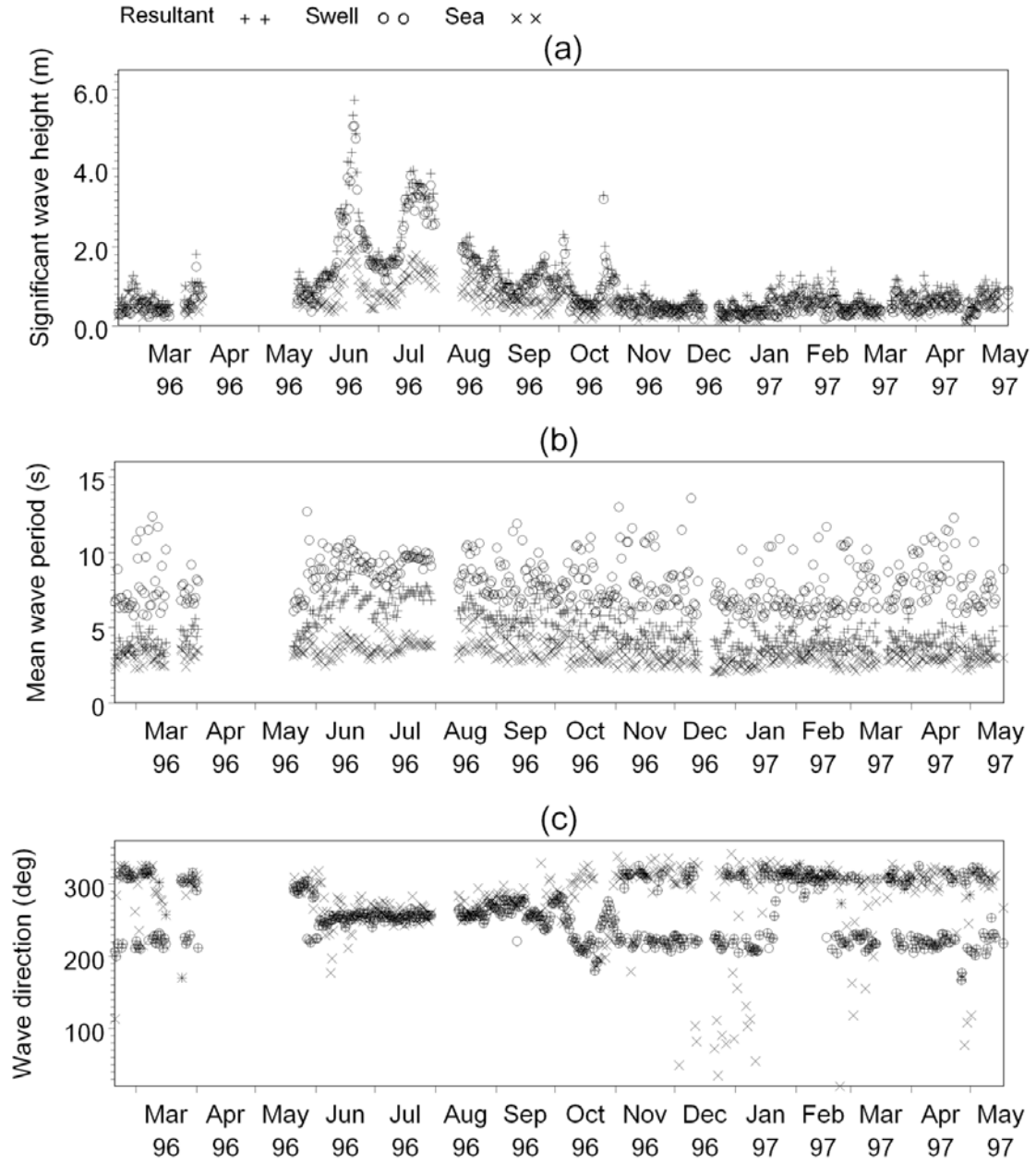


Figure 4

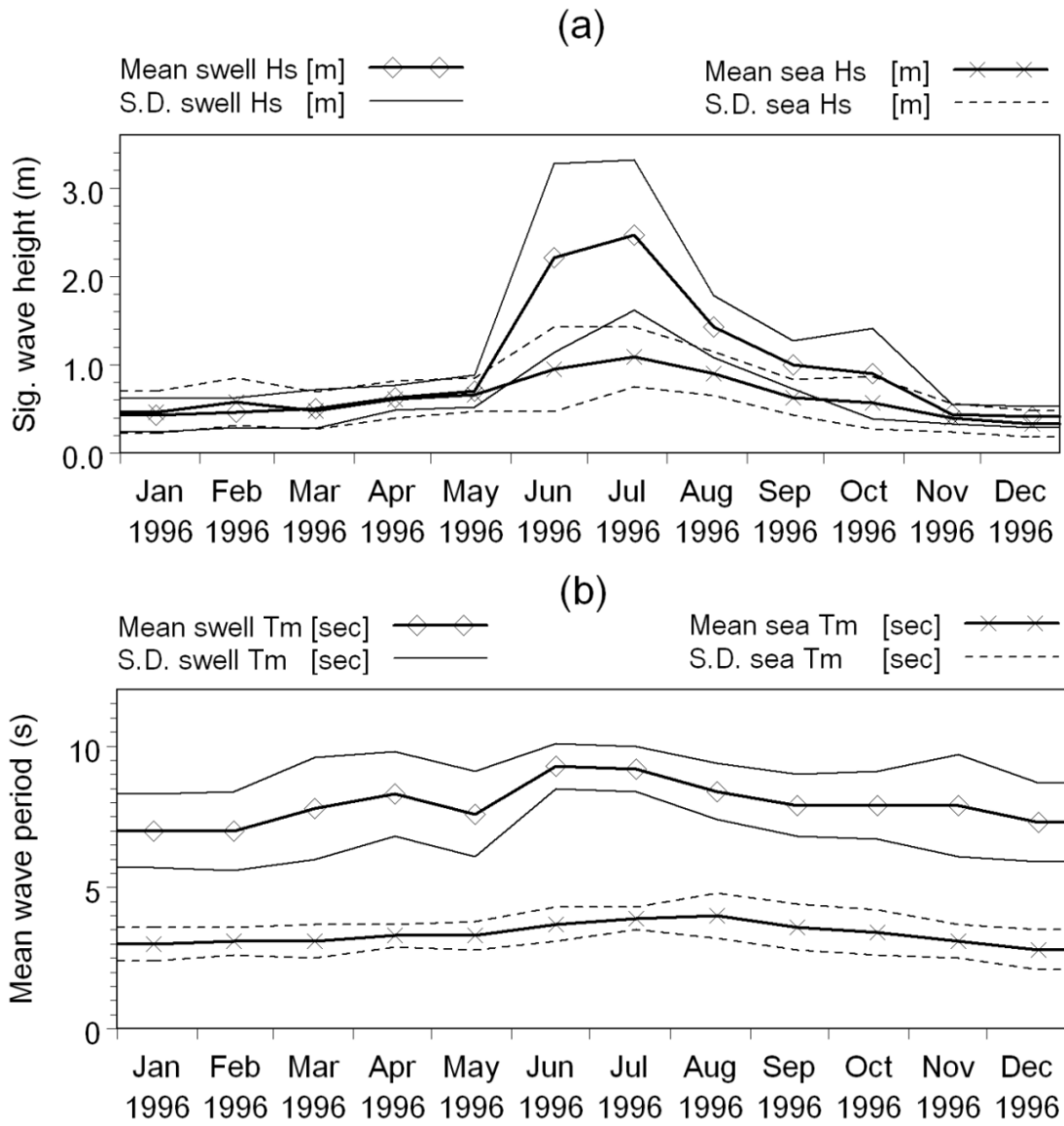


Figure 5

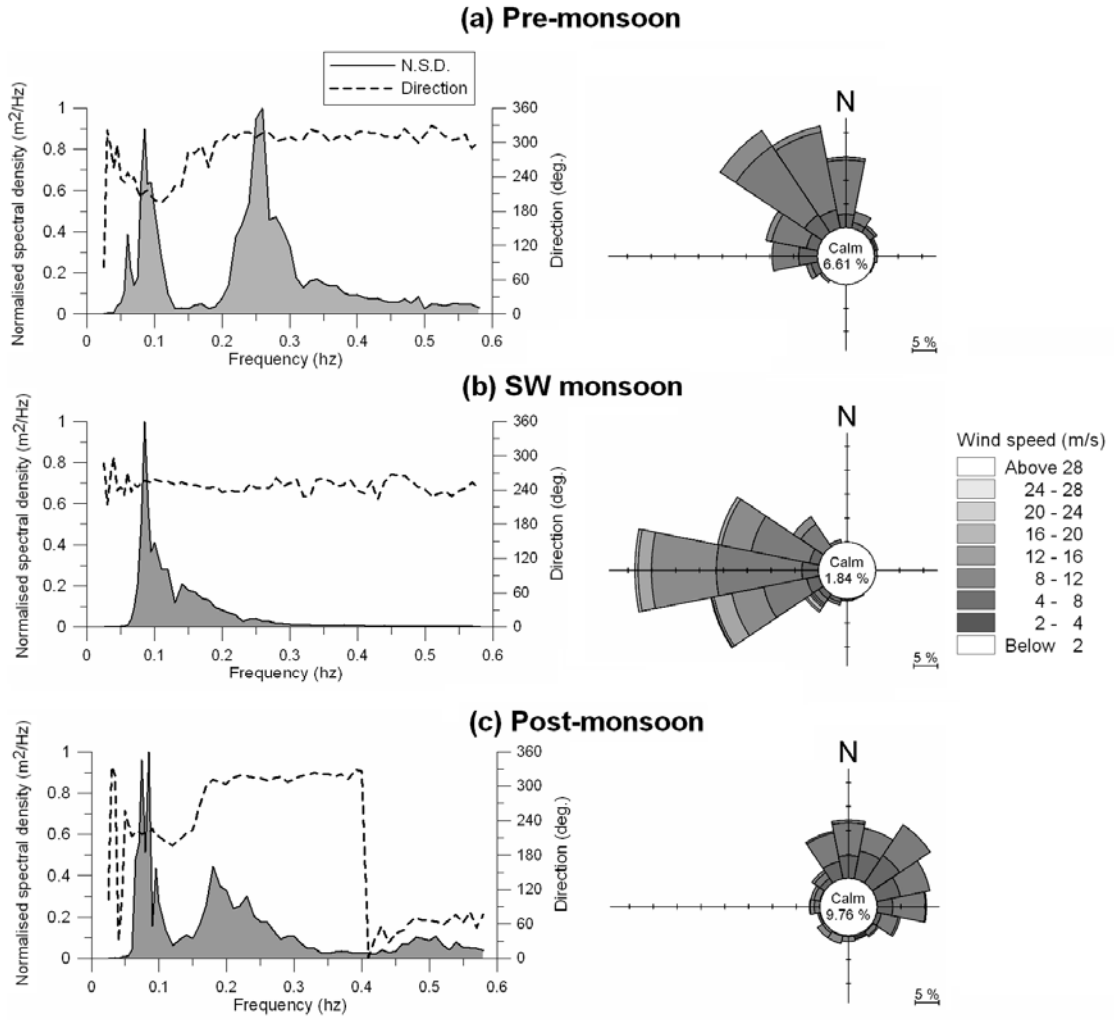


Figure 6

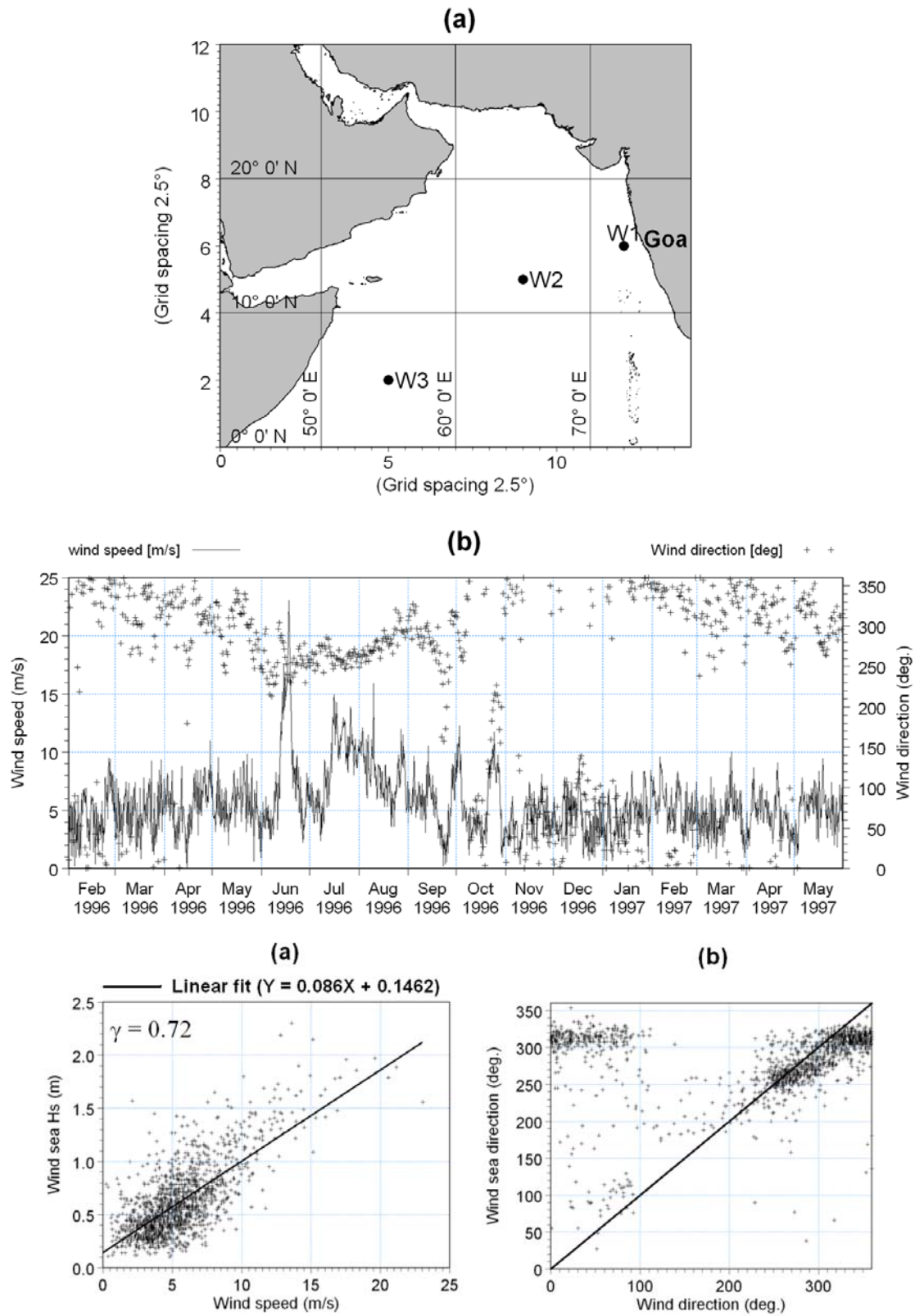


Figure 7

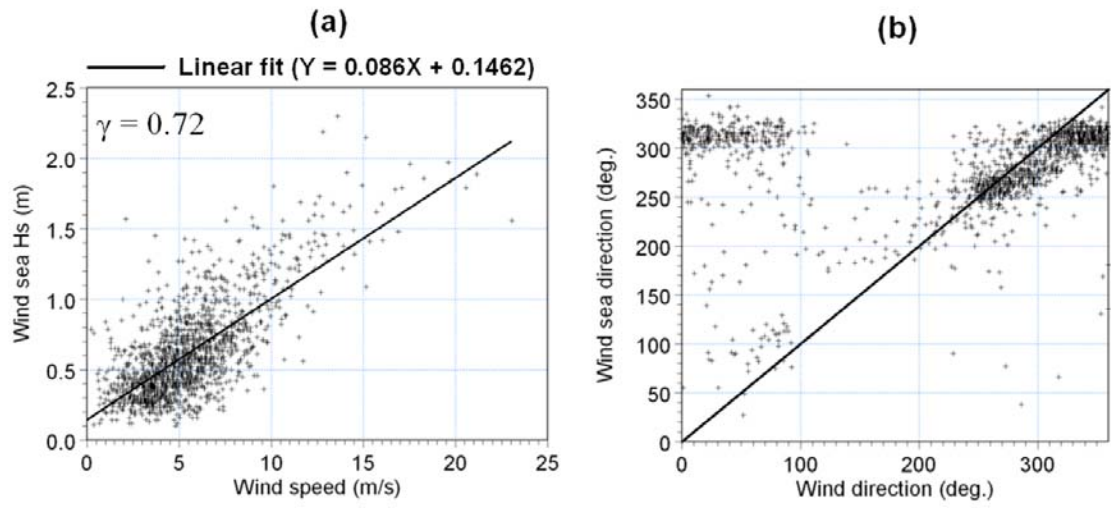


Figure 8

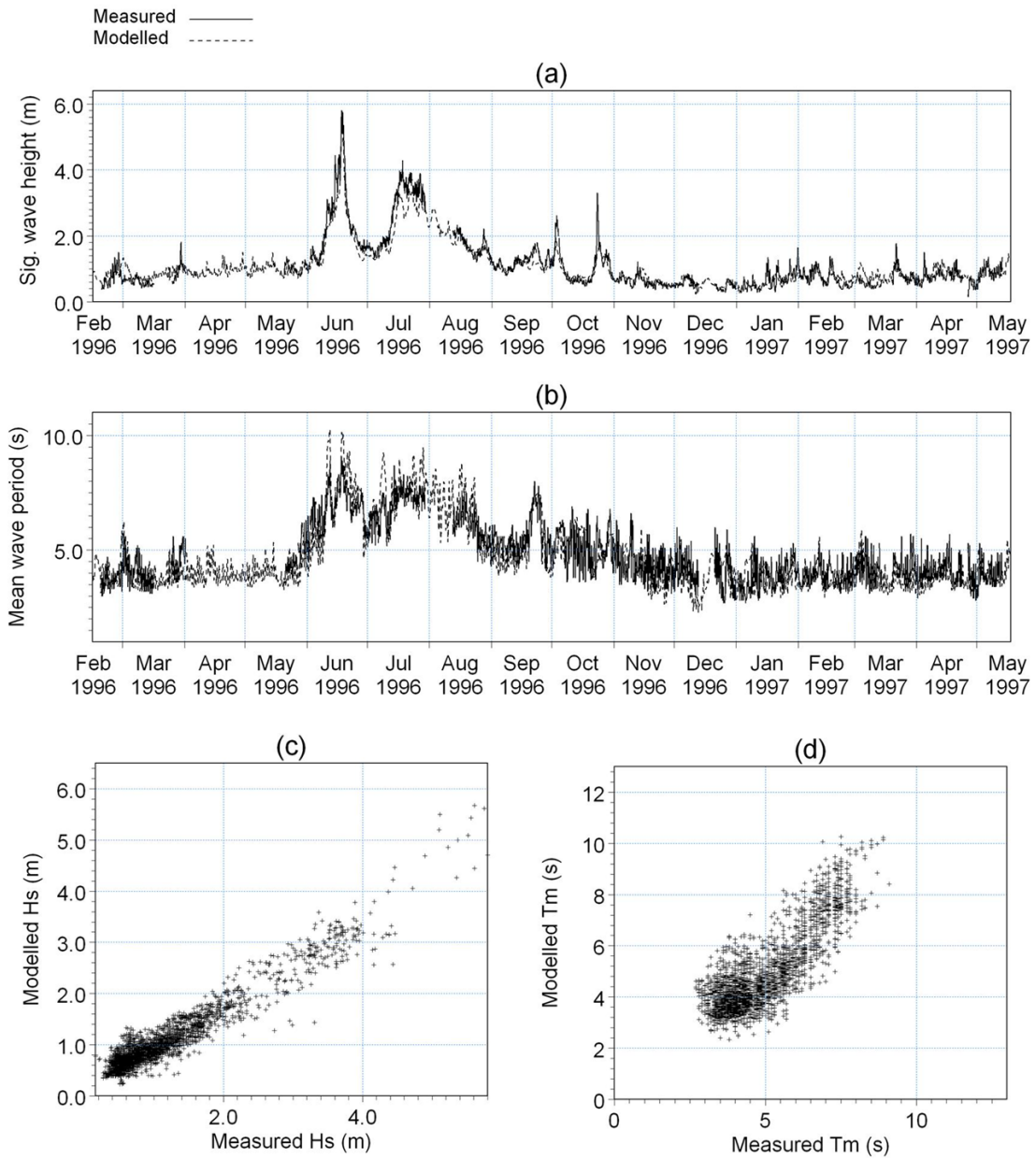


Figure 9

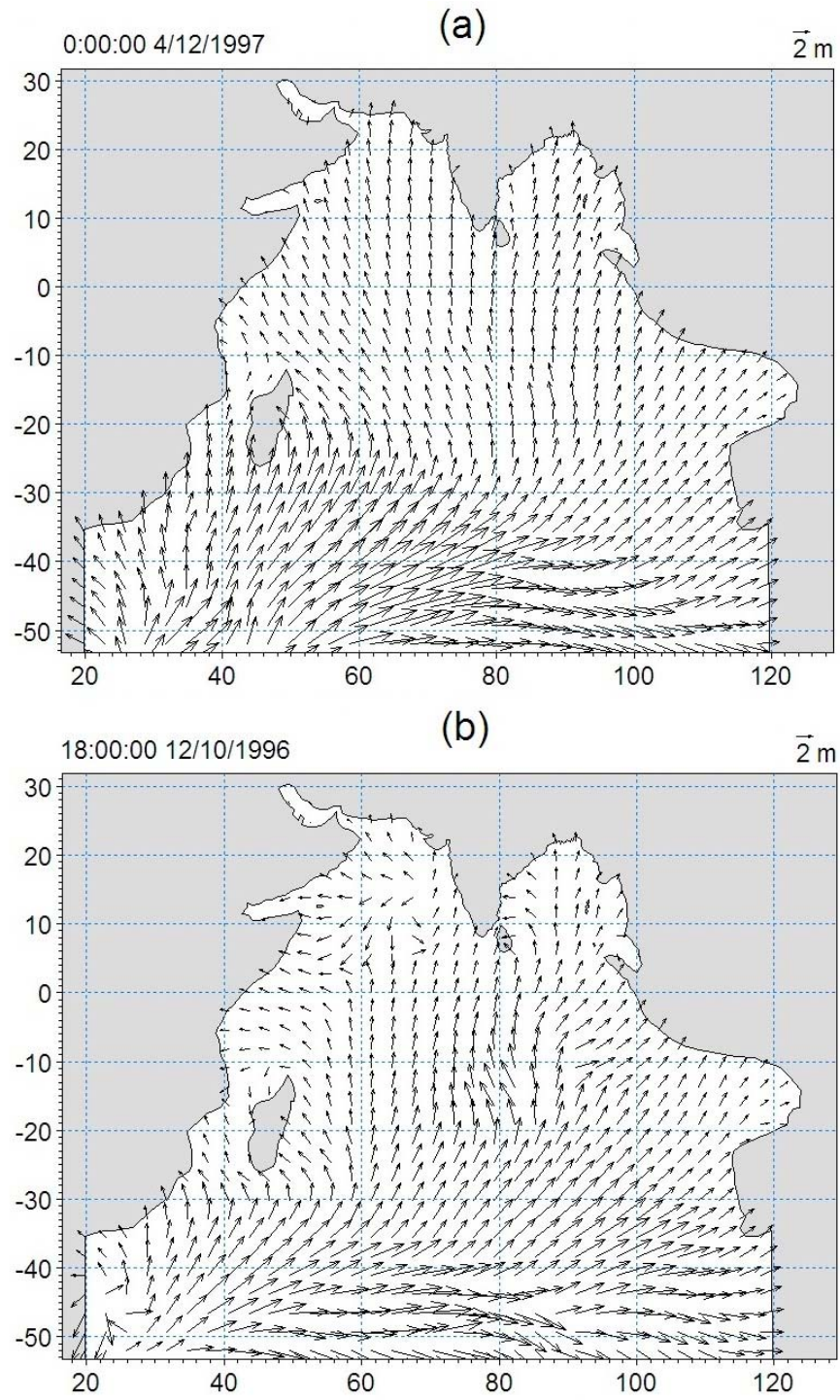


Figure 10

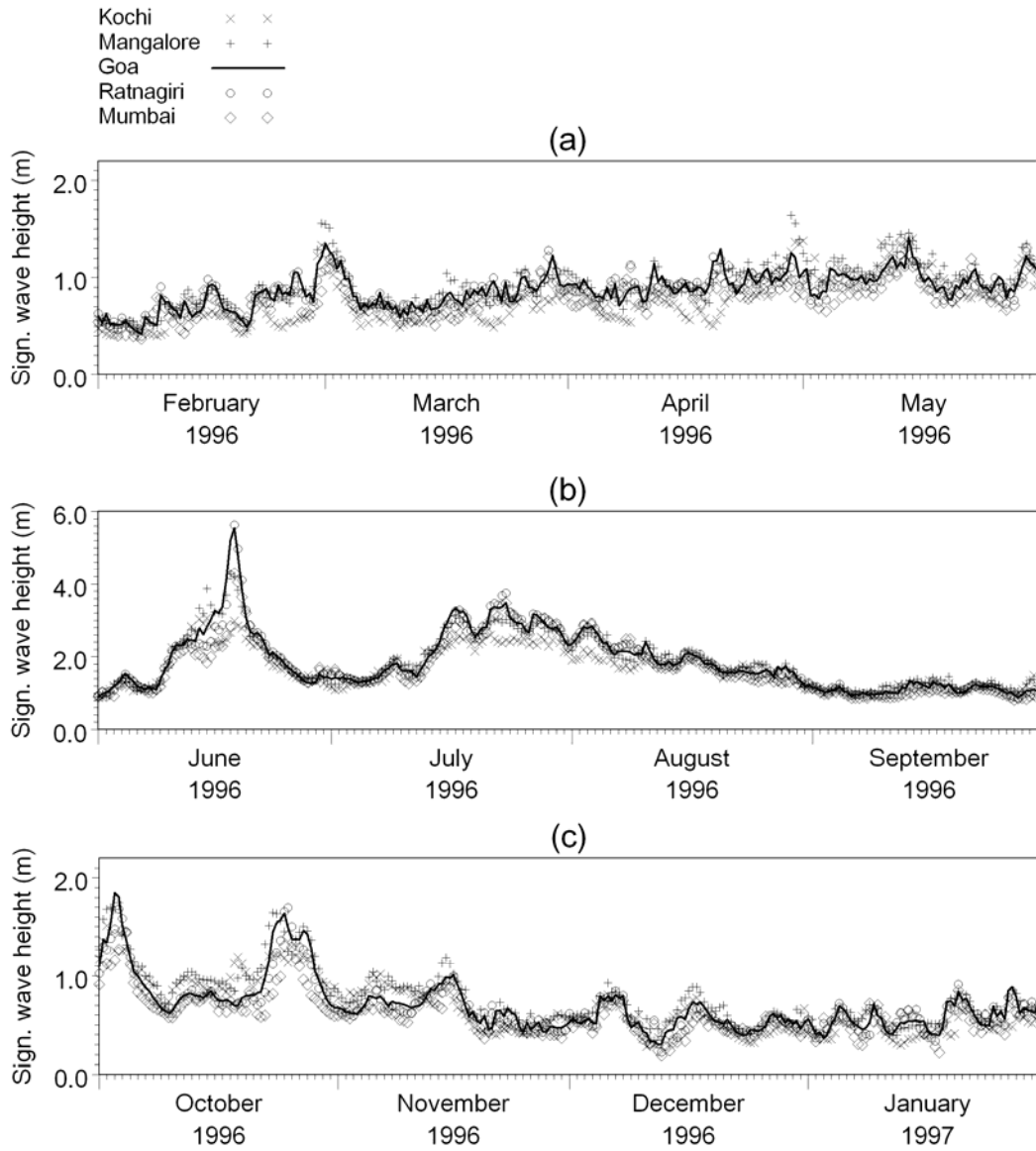


Figure 11



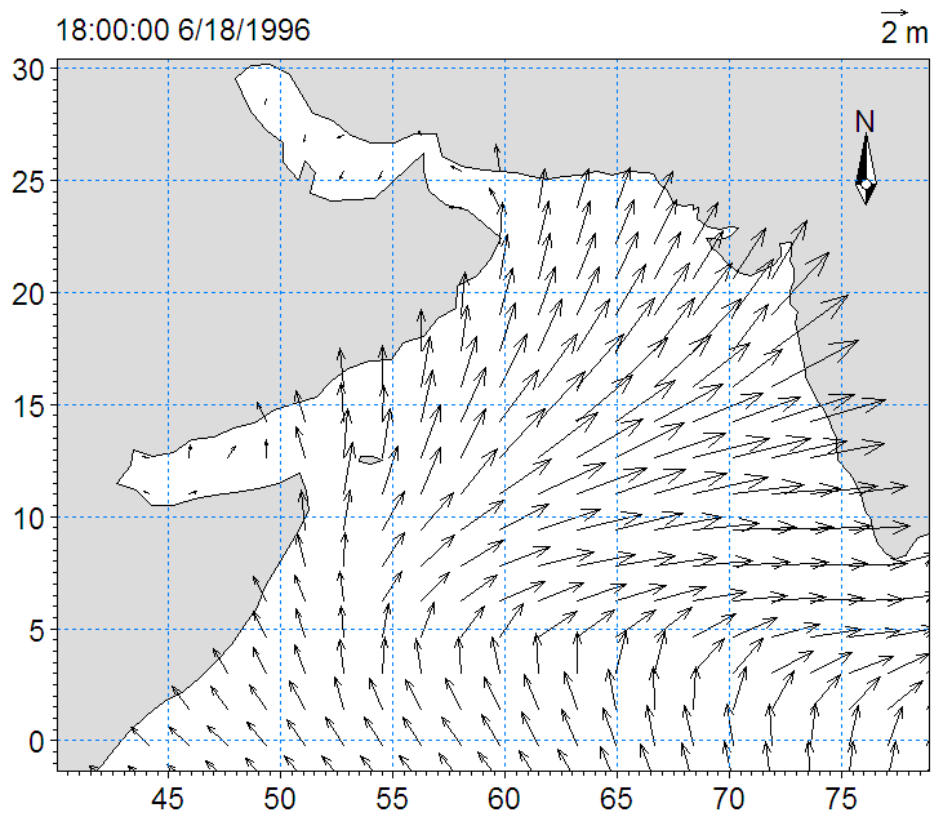


Figure 12